

# Recycling of $\text{Li}_2\text{ZrO}_3$ as $\text{LiCl}$ and $\text{ZrO}_2$ via a Chlorination Technique

Min Ku Jeon<sup>1,2,\*</sup>, Sung-Wook Kim<sup>1</sup>, Keun-Young Lee<sup>1</sup>, and Eun-Young Choi<sup>1,2</sup>

<sup>1</sup>*Korea Atomic Energy Research Institute, 111, Daedeok-daero 989beon-gil, Yuseong-gu, Daejeon 34057, Republic of Korea*

<sup>2</sup>*University of Science and Technology, 217, Gajeong-ro, Yuseong-gu, Daejeon 34113, Republic of Korea*

(Received February 10, 2021 / Revised March 8, 2021 / Approved March 12, 2021)

In this study, a chlorination technique for recycling  $\text{Li}_2\text{ZrO}_3$ , a reaction product of  $\text{ZrO}_2$ -assisted rinsing process, was investigated to minimize the generation of secondary radioactive pyroprocessing waste. It was found that the reaction temperature was a key parameter that determined the reaction rate and maximum conversion ratio. In the temperature range of 400–600°C, an increase in the reaction temperature resulted in a profound increase in the reaction rate. Hence, according to the experimental results, a reaction temperature of at least 450°C was proposed to ensure a  $\text{Li}_2\text{ZrO}_3$  conversion ratio that exceeded 80% within 8 h of the reaction time. The activation energy was found to be  $102 \pm 2 \text{ kJ}\cdot\text{mol}^{-1}\cdot\text{K}^{-1}$  between 450 and 500°C. The formation of  $\text{LiCl}$  and  $\text{ZrO}_2$  as reaction products was confirmed by X-ray diffraction analysis. The experimental results obtained at various total flow rates revealed that the overall reaction rate depends on the  $\text{Cl}_2$  mass transfer rate in the experimental condition. The results of this study prove that the chlorination technique provides a solution to minimize the amount of radioactive waste generated during the  $\text{ZrO}_2$ -assisted rinsing process.

Keywords: Chlorination reaction, Oxide reduction, Lithium zirconate, Lithium chloride, Molten salt rinsing

\*Corresponding Author.

Min Ku Jeon, Korea Atomic Energy Research Institute, E-mail: [minku@kaeri.re.kr](mailto:minku@kaeri.re.kr), Tel: +82-42-868-2435

## ORCID

Min Ku Jeon

<http://orcid.org/0000-0001-8115-3241>

Sung-Wook Kim

<http://orcid.org/0000-0002-5537-4793>

Keun-Young Lee

<http://orcid.org/0000-0001-7144-9014>

Eun-Young Choi

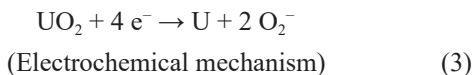
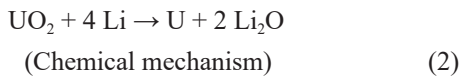
<http://orcid.org/0000-0003-1693-7642>

## 1. Introduction

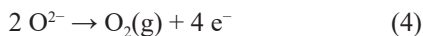
Oxide reduction (OR) is a key process that enables the use of oxide fuels discharged from pressurized water reactors (PWRs) in electrochemical pyroprocessing [1]. Recycling of the metallic fuels, employed in the Experimental Breeder Reactor-II (EBR-II) sodium-cooled fast reactor (SFR), via pyroprocessing was successfully demonstrated in the USA [2]. An integrated system of pyroprocessing and SFR is under intensive research in South Korea with the aim of recycling the transuranic (TRU) nuclides existing in the used nuclear fuels (UNFs) of PWRs as a fuel for SFRs [3-4].

The OR process liberates oxygen atoms from oxide fuels so that the resulting metallic fuels can be processed via subsequent electro-refining and electro-winning processes to recover U and TRU nuclides. Normally,  $\text{LiCl}$  containing 1-3wt%  $\text{Li}_2\text{O}$  is employed as a molten salt in the OR process at around  $650^\circ\text{C}$  [5-8]. In order to construct an electrochemical circuit for the OR process, oxide fuels are loaded into a metal basket to serve as the cathode, with platinum employed as the anode. The reactions occurring at the cathode and anode are listed below:

<Cathode>



<Anode>

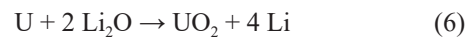


There are two mechanisms, chemical and electrochemical, which explain the reaction behavior at the cathode. In the chemical mechanism, Li metal is generated through reaction (1) and then reacts with  $\text{UO}_2$  to produce U and  $\text{Li}_2\text{O}$

via reaction (2). In the electrochemical mechanism,  $\text{UO}_2$  is directly converted to U via an electrochemical reaction (3). As the operation potential of the two mechanisms are close, both pathways can occur simultaneously during the OR operation. In the anode, oxygen ions liberated from  $\text{UO}_2$  are oxidized to  $\text{O}_2$  gas through reaction (4). Regardless of the cathode reaction mechanism, the overall reaction equation of the OR process can be expressed as reaction (5).



When the OR operation is complete, the cathode basket is discharged from the reactor along with any residual salt adhering to the metallic fuel and basket. The cathode basket is transferred to a salt distillation process, during which the residual salt is removed by heat and a vacuum to obtain clean metallic fuel [3, 4, 9]. During this process,  $\text{Li}_2\text{O}$  dissolved in the residual salt reacts with U metal, resulting in a reoxidation reaction through reaction (6), expressed below, which is a reverse reaction of reaction (2) [10, 11].

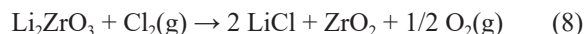


Here, the consistent removal of Li, with a melting point of 454 K and a boiling point of 1615 K, using heat and a vacuum is a key driving force that keeps reaction (6) going. In addition, it was documented that a higher  $\text{Li}_2\text{O}$  concentration or distillation temperature can lead to a higher degree of reoxidation [10, 11].

This reoxidation phenomenon will cause a significant reduction in the overall process efficiency, as the reoxidized product,  $\text{UO}_2$ , is not recoverable through electro-refining. Recently, Choi et al. proposed a  $\text{ZrO}_2$ -assisted rinsing process as an alternative to the salt distillation process [12]. In this process, the cathode basket is immersed in a separate bath of molten  $\text{LiCl}$  such that  $\text{Li}_2\text{O}$  in the residual salt is diluted. Here,  $\text{ZrO}_2$  is utilized as a  $\text{Li}_2\text{O}$  scavenger to prevent the accumulation of  $\text{Li}_2\text{O}$  in the rinsing bath via the following reaction mechanism [13, 14]:



Although the rinsing technique was successfully demonstrated through repeated experiments, the reaction product,  $\text{Li}_2\text{ZrO}_3$ , should be replaced by  $\text{ZrO}_2$  periodically. The resulting  $\text{Li}_2\text{ZrO}_3$  can be handled as a radioactive waste for disposal after several treatments. As a result, the  $\text{ZrO}_2$ -assisted rinsing technique will produce additional radioactive waste,  $\text{Li}_2\text{ZrO}_3$ , unless it can be recycled. In this work, a chlorination technique was applied to recycle  $\text{Li}_2\text{ZrO}_3$  through reaction (8) below, with the goal of recycling  $\text{LiCl}$  and  $\text{ZrO}_2$  in the  $\text{ZrO}_2$ -assisted rinsing process.



## 2. Experimental

The Gibbs free energy change ( $\Delta G$ ) values of the  $\text{Li}_2\text{ZrO}_3$  chlorination reaction (reaction (8)) were derived using the HSC chemistry software (version 9.5.1) as a function of the reaction temperature [15]. Chlorination experiments were conducted using a quartz tube reactor with a diameter of 4 cm. The reactor was equipped with an electrical furnace to control the reaction temperature. Before the reaction began, the weight of the  $\text{Li}_2\text{ZrO}_3$  powder (Sigma-Aldrich) was measured before and after the sample was loaded into an alumina boat. Approximately 0.50 g of  $\text{Li}_2\text{ZrO}_3$  was used for each experiment. The boat was placed in the middle of the quartz reactor and both ends were then connected to a gas control system. On the inlet side of the reactor, a gas feed system with two mass flow controllers (MFCs, Kofloc co., Japan) for Ar (Model 3660) and  $\text{Cl}_2$  (Model 5440) was connected. A dry scrubbing system for the removal of unreacted  $\text{Cl}_2$  was connected to the other side of the reactor. After purging the reactor with Ar for at least 2 h, the reactor was heated to the reaction temperature at a ramping rate of  $10^\circ\text{C}\cdot\text{min}^{-1}$  under an argon flow. When the reactor temperature is settled at the target temperature, each MFC

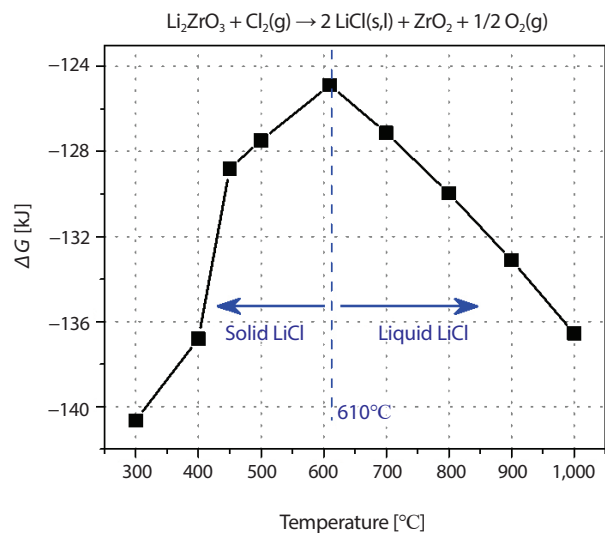


Fig. 1.  $\Delta G$  values of the reaction between  $\text{Li}_2\text{ZrO}_3$  and  $\text{Cl}_2$  (Eq. 8) at various temperatures calculated using the HSC chemistry software.

was set at the reaction flow rate and then maintained for the reaction time. Upon the completion of the reaction, the  $\text{Cl}_2$  flow was stopped and the reactor was cooled to room temperature under an argon flow. After discharging the alumina boat, the weight of the sample was measured with or without the alumina boat to quantify the weight change. The highest reaction temperature in this work was set to  $600^\circ\text{C}$  in order to minimize the volatilization loss of  $\text{LiCl}$  during the reaction. Experiments were repeated for various reaction temperatures ( $300\text{--}600^\circ\text{C}$ ), durations, and total flow rates ( $Q = \text{sum of the Ar and } \text{Cl}_2 \text{ flow rates}$ ).

The phase change of the samples was analyzed using an X-ray diffraction system (XRD, Bruker D8 Advance). The analysis was conducted in the  $2\theta$  range of  $10\text{--}80^\circ$  with a step size of  $0.0104^\circ$  and measurement time of 0.15 s during each step.

## 3. Results and discussion

The  $\Delta G$  values of the  $\text{Li}_2\text{ZrO}_3$  chlorination reaction were derived using the HSC chemistry software. These results

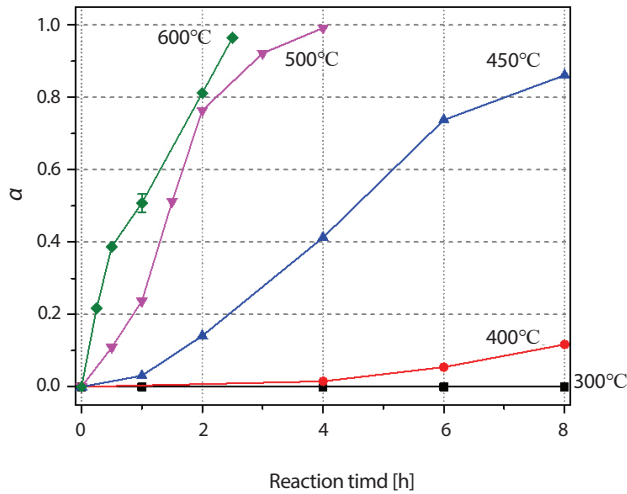


Fig. 2. Experimental results obtained at various reaction temperatures and times with a flow rate of 98 mL·min<sup>-1</sup> Ar + 2 mL·min<sup>-1</sup> Cl<sub>2</sub>.

are shown in Fig. 1. The ΔG value represents the change in the chemical potential when the reaction proceeds, which is negative when the sum of the chemical potentials of the reaction products is smaller than that of the reactants. In other words, a negative ΔG indicates that the reaction is thermodynamically feasible. In Fig. 1, negative ΔG values were observed throughout the temperature range (300–1,000°C), suggesting that the Li<sub>2</sub>ZrO<sub>3</sub> chlorination reaction is thermodynamically feasible. The volcano shape of the figure came from phase change of LiCl from a solid to a liquid at 610°C, which is the melting point of LiCl. The following equation, where ΔH and ΔS correspondingly represent changes in enthalpy and entropy, accounts for the volcano shape because the melting of LiCl leads to an increase in the ΔS value.

$$\Delta G = \Delta H - T\Delta S \tag{9}$$

However, an experimental approach should be utilized in order to verify the actual operating temperature as the activation energy and rate of the reaction are not included in the ΔG values.

The effects of the reaction temperatures and times were also investigated, as shown in Fig. 2. In the figure, the term

α, the conversion ratio, is noted, representing the ratio of Li<sub>2</sub>ZrO<sub>3</sub> reacted with Cl<sub>2</sub> over the input of Li<sub>2</sub>ZrO<sub>3</sub>. This value was calculated using the following equation,

$$\alpha = \frac{(W_f - W_i) / (W_i)}{((2 \times M.W_{LiCl} + M.W_{ZrO_2} - M.W_{Li_2ZrO_3}) / M.W_{Li_2ZrO_3})} \tag{10}$$

where W<sub>f</sub> and W<sub>i</sub> represent the final and initial weight of the samples, respectively, and M.W<sub>LiCl</sub>, M.W<sub>ZrO<sub>2</sub></sub>, and M.W<sub>Li<sub>2</sub>ZrO<sub>3</sub></sub> correspondingly represent the molecular weight of LiCl (= 42.39 g·mol<sup>-1</sup>), ZrO<sub>2</sub> (=123.2 g·mol<sup>-1</sup>), and Li<sub>2</sub>ZrO<sub>3</sub> (= 153.1 g·mol<sup>-1</sup>). Interestingly, no signs of the reaction were found at 300°C, while the reaction proceeded slightly at 400°C (α = 0.117 after 8 h of reaction). It is clear here that the reaction temperature should be at least 400°C to overcome the activation energy of the Li<sub>2</sub>ZrO<sub>3</sub> chlorination reaction, although the reaction is very slow at 400°C. In addition, this outcome shows why the experimental approach should be used in conjunction with thermodynamic calculations. With an increase in the reaction temperature to 450 and 500°C, a profound increase in α was observed. The reaction was found to be complete after 4 h at 500°C. A further increase in the reaction temperature to 600°C brought a significant increase in the value of α, especially in the region of α ≤ 0.5. It is obvious from this result that the reaction temperature is a key parameter which determines the reaction rate and maximum value of α, especially in the temperature range of 400–600°C. Reproducibility of the experiments was verified by repeating identical experiments three times at 600°C for 1 h under a 98 mL·min<sup>-1</sup> Ar + 2 mL·min<sup>-1</sup> Cl<sub>2</sub> flow. These results are shown the error bar in Fig. 2, where the resulting α value was 0.508 ± 0.025. This outcome proves the acceptable reproducibility of the experiments conducted in this work.

Activation energy of the Li<sub>2</sub>ZrO<sub>3</sub> chlorination reaction was derived using the data of Fig. 2. In a gas-solid reaction, the reaction rate can be expressed using the following equation,

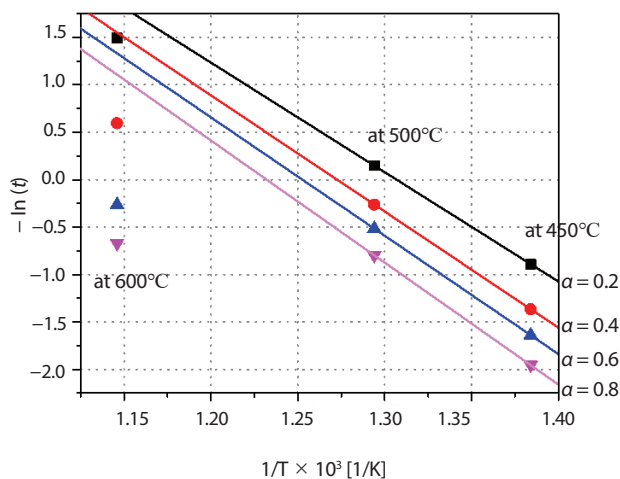


Fig. 3. Plot of  $-\ln(t)$  versus  $1/T \times 10^3$  for the calculation of activation energy at  $\alpha$  values of 0.2, 0.4, 0.6, and 0.8 under a  $98 \text{ mL} \cdot \text{min}^{-1}$  Ar +  $2 \text{ mL} \cdot \text{min}^{-1}$   $\text{Cl}_2$  flow.

$$R = \frac{d\alpha}{dt} = k(T)F(p\text{Cl}_2)G(\alpha) \quad (11)$$

where  $k(T)$ ,  $F(p\text{Cl}_2)$ , and  $G(\alpha)$  represent the effects of reaction temperature, chlorine partial pressure, and morphological changes, respectively. Applying the Arrhenius equation in  $k(T)$  and integration of Eq. (11) results in the following equation,

$$-\ln(t) = C(\alpha) - \frac{E_a}{R_g} \frac{1}{T} \quad (12)$$

where  $C(\alpha)$  represents combination of  $F(p\text{Cl}_2)$  and  $G(\alpha)$  at a constant  $p\text{Cl}_2$ ,  $E_a$  is an activation energy, and  $R_g$  is the gas constant ( $8.314 \text{ J} \cdot \text{mol}^{-1} \cdot \text{K}^{-1}$ ). Here, the  $E_a$  value can be derived from the slope of  $-\ln(t)$  versus  $1/T$  plot for a given  $\alpha$ . The experimental results at  $\alpha$  values of 0.2, 0.4, 0.6, and 0.8 are shown in Fig. 3 with linear fitting results. Here, linear interpolation was applied to the  $\alpha$  and  $t$  values. It should be noted that the results at  $600^\circ\text{C}$  were not included in the linear fitting calculations because of significant discrepancy in the trend. The activation energy calculated from the results at 450 and  $500^\circ\text{C}$  was  $102 \pm 2 \text{ kJ} \cdot \text{mol}^{-1} \cdot \text{K}^{-1}$ . These results also propose that the reaction regime is changing between 500 and  $600^\circ\text{C}$ .

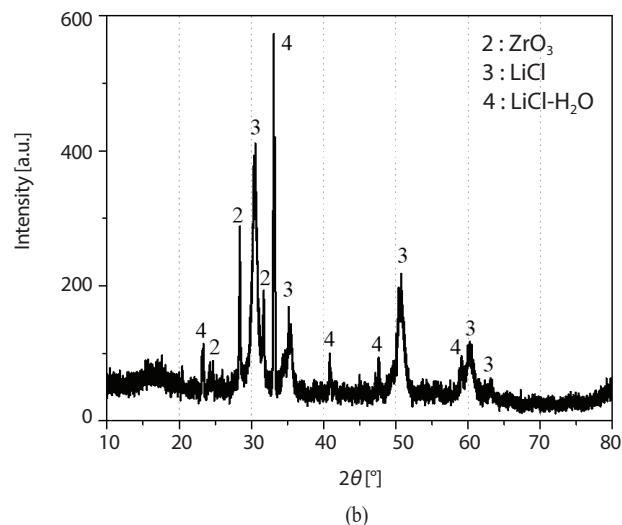
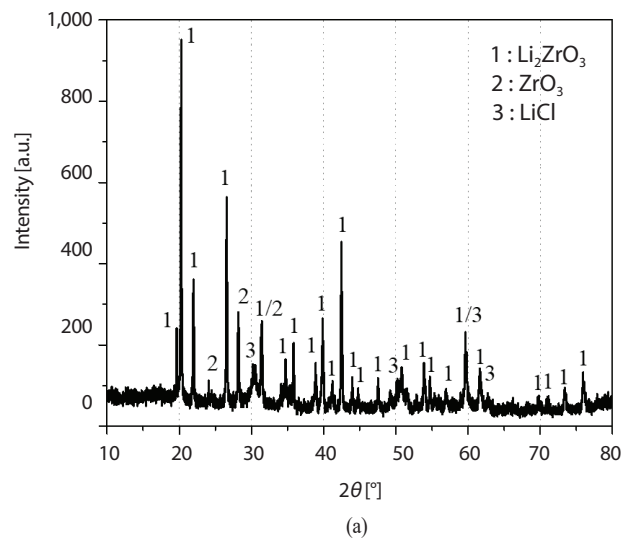


Fig. 4. XRD measurement results of  $\text{Li}_2\text{ZrO}_3$  reacted at  $500^\circ\text{C}$  for (a) 1.0 and (b) 4.0 h under a  $98 \text{ mL} \cdot \text{min}^{-1}$  Ar +  $2 \text{ mL} \cdot \text{min}^{-1}$   $\text{Cl}_2$  flow.

Phase changes in the samples prepared at  $500^\circ\text{C}$  for 1.0 and 4.0 h were analyzed by XRD measurements, as shown in Fig. 4. After 1.0 h of the reaction ( $\alpha = 0.2374$ ), the XRD peaks could be assigned according to the three phases of  $\text{Li}_2\text{ZrO}_3$  (PDF #01-070-8744),  $\text{ZrO}_2$  (PDF #01-078-0047), and  $\text{LiCl}$  (PDF #01-074-1972). Peaks of  $\text{Li}_2\text{ZrO}_3$  were not observed after 4.0 h of the reaction ( $\alpha = 0.9922$ ), as shown in Fig. 4(b), whereas peaks of  $\text{LiCl} \cdot \text{H}_2\text{O}$  (PDF #01-070-9971) were noted. Considering the hygroscopic characteristic of

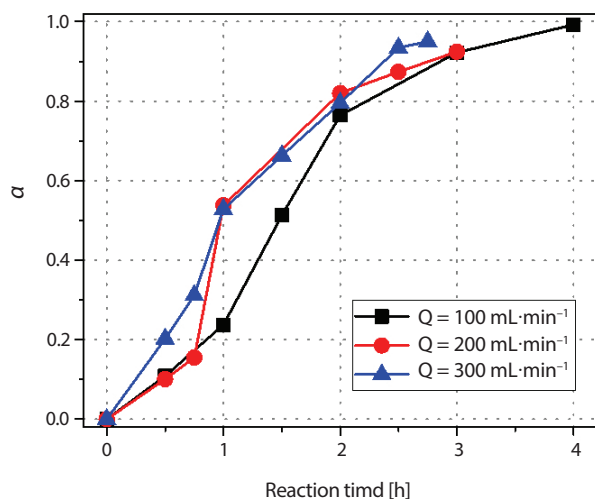


Fig. 5. Experimental results obtained at  $500^\circ\text{C}$  for various  $Q$  values of 100 ( $= 98 \text{ mL}\cdot\text{min}^{-1} \text{ Ar} + 2 \text{ mL}\cdot\text{min}^{-1} \text{ Cl}_2$ ), 200 ( $= 196 \text{ mL}\cdot\text{min}^{-1} \text{ Ar} + 4 \text{ mL}\cdot\text{min}^{-1} \text{ Cl}_2$ ), and  $300 \text{ mL}\cdot\text{min}^{-1}$  ( $294 \text{ mL}\cdot\text{min}^{-1} \text{ Ar} + 6 \text{ mL}\cdot\text{min}^{-1} \text{ Cl}_2$ ).

$\text{LiCl}$ , the  $\text{LiCl}\text{-H}_2\text{O}$  phase may have been generated during the sample handling process for the XRD measurements. These outcomes prove that the weight-based calculation of  $\alpha$  was a reasonable approach for the experiments conducted at  $500^\circ\text{C}$ , assuming that the weight was measured as soon as the samples were exposed to air. In addition, the absence of unexpected reaction by-products was confirmed by XRD measurement results.

In a solid-gas reaction system, the reaction rate is controlled by either or both of mass transfer rate of gas,  $\text{Cl}_2$  in this work, and chemical reaction rate. Under a mass transfer rate controlled condition, an increase in the  $Q$  value leads to an increase in the reaction rate because the amount that is transferred to the surface of reactant,  $\text{Li}_2\text{ZrO}_3$ , affects the overall reaction rate. On the other hand, the reaction rate is independent of  $Q$  under the chemical reaction rate controlled condition. In order to identify the reaction mechanism of this work, the effect of  $Q$  at  $500^\circ\text{C}$  was investigated by repeating experiments under various flow rates of  $98 \text{ mL}\cdot\text{min}^{-1} \text{ Ar} + 2 \text{ mL}\cdot\text{min}^{-1} \text{ Cl}_2$  ( $Q = 100 \text{ mL}\cdot\text{min}^{-1}$ ),  $196 \text{ mL}\cdot\text{min}^{-1} \text{ Ar} + 4 \text{ mL}\cdot\text{min}^{-1} \text{ Cl}_2$  ( $Q = 200 \text{ mL}\cdot\text{min}^{-1}$ ), and  $294 \text{ mL}\cdot\text{min}^{-1} \text{ Ar} + 6 \text{ mL}\cdot\text{min}^{-1} \text{ Cl}_2$  ( $Q = 300 \text{ mL}\cdot\text{min}^{-1}$ ) for various

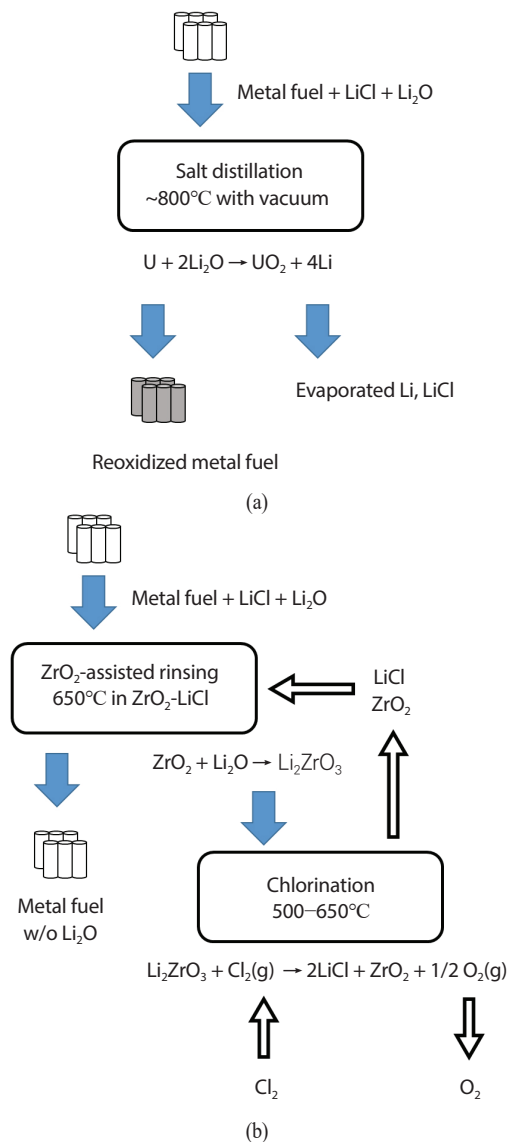


Fig. 6. Flow diagrams of (a) the conventional salt distillation process and (b) the  $\text{ZrO}_2$ -assisted rinsing process combined with  $\text{Li}_2\text{ZrO}_3$  chlorination.

reaction times as shown in Fig. 5. Note that the ratio of  $\text{Cl}_2$  was kept constant at 2% of  $Q$  in order to eliminate the effect of  $\text{Cl}_2$  partial pressure. In the figure, an increase in the  $Q$  value leads to an increase in the reaction rate suggesting that the reaction is under the influence of  $\text{Cl}_2$  mass transfer rate at  $500^\circ\text{C}$ . It is interesting to observe the results with  $Q$  of  $200 \text{ mL}\cdot\text{min}^{-1}$ , which exhibited similar values to those with  $100 \text{ mL}\cdot\text{min}^{-1}$  in the low ( $< 0.2$ ) and high ( $> 0.9$ )  $\alpha$  regions,



and with  $300 \text{ mL}\cdot\text{min}^{-1}$  in the middle ( $0.5 < \alpha < 0.85$ ) region. Here, it is worth to note that the reaction time for high conversion ( $> 90\%$ ) reduced less significantly, though it is clear that an increase in  $Q$  accelerates the reaction rate under the condition of this work.

A combined flow diagram of the  $\text{ZrO}_2$ -assisted rinsing and  $\text{Li}_2\text{ZrO}_3$  chlorination processes is displayed in Fig. 6 in comparison with the conventional salt distillation process. The concept of combining the  $\text{ZrO}_2$ -assisted rinsing and chlorination processes involves the use of  $\text{ZrO}_2$ -dispersed  $\text{LiCl}$  salt during the rinsing process. After a certain level of  $\text{ZrO}_2$  is converted into  $\text{Li}_2\text{ZrO}_3$  by reacting with  $\text{Li}_2\text{O}$ , bubbling chlorine gas through the rinsing salt can eliminate the need for a separate reactor for the chlorination process. When scaling up these processes, the bath size and the  $\text{ZrO}_2$  input of the rinsing process may be the key parameters determining the capacity of the rinsing bath and frequency of  $\text{Li}_2\text{ZrO}_3$  chlorination. In addition, various aspects such as the process cost, operation time, and total process efficiency should be compared between the conventional salt distillation process and the  $\text{ZrO}_2$ -assisted rinsing step combined with the chlorination process.

## 4. Conclusions

A chlorination reaction of  $\text{Li}_2\text{ZrO}_3$  to recycle it as  $\text{LiCl}$  and  $\text{ZrO}_2$  via a  $\text{ZrO}_2$ -assisted rinsing process was successfully demonstrated in various experiments. It was found that the reaction temperature is a key parameter of the reaction to achieve a high conversion ratio, suggesting an operating temperature of at least  $450^\circ\text{C}$ . The activation energy was estimated to be  $102 \pm 2 \text{ kJ}\cdot\text{mol}^{-1}\cdot\text{K}^{-1}$  at  $450$  and  $500^\circ\text{C}$ . The effect of  $Q$  on the  $\alpha$  value at  $500^\circ\text{C}$  indicated that the reaction rate of this study is under control of  $\text{Cl}_2$  mass transfer rate under the condition of this work. The outcomes of this work suggest that the chlorination technique can solve the problem of extra waste ( $\text{Li}_2\text{ZrO}_3$ ) generation during the  $\text{ZrO}_2$ -assisted rinsing process.

## Acknowledgements

This work was sponsored by the Nuclear R&D program of the Korean Ministry of Science and ICT (2017M2A8A5015147 and 2017M2A8A5015077).

## REFERENCES

- [1] S.D. Herrmann and S.X. Li, "Separation and Recovery of Uranium Metal From Spent Light Water Reactor Fuel Via Electrolytic Reduction and Electrorefining", *Nucl. Technol.*, 171(3), 247-265 (2010).
- [2] C.E. Stevenson, *The EBR-II Fuel Cycle Story*, 53-198, La Grange park, Illinois, 1987.
- [3] K.C. Song, H. Lee, J.M. Hur, J.G. Kim, D.H. Ahn, and Y.Z. Cho, "Status of Pyroprocessing Technology Development in Korea", *Nucl. Eng. Technol.*, 42(2), 131-144 (2010).
- [4] H. Lee, G.I. Park, K.H. Kang, J.M. Hur, J.G. Kim, D.H. Ahn, Y.Z. Cho, and E.H. Kim, "Pyroprocessing Technology Development at KAERI", *Nucl. Eng. Technol.*, 43(4), 317-328 (2011).
- [5] S.D. Herrmann, S.X. Li, M.F. Simpson, and S. Phongikaroon, "Electrolytic Reduction of Spent Nuclear Oxide Fuels as Part of an Integral Process to Separate and Recover Actinides From Fission Products", *Sep. Sci. Technol.*, 41(10), 1965-1983 (2006).
- [6] Y. Sakamura and T. Omori, "Electrolytic Reduction and Electrorefining of Uranium to Develop Pyrochemical Reprocessing of Oxide Fuels", *Nucl. Technol.*, 171(3), 266-275 (2010).
- [7] E.Y. Choi, J. Lee, D.H. Heo, S.K. Lee, M.K. Jeon, S.S. Hong, S.W. Kim, H.W. Kang, S.C. Jeon, and J.M. Hur, "Electrolytic Reduction Runs of 0.6 kg Scale-Simulated Oxide Fuel in a  $\text{Li}_2\text{O}$ - $\text{LiCl}$  Molten Salt Using Metal Anode Shrouds", *J. Nucl. Mater.*, 489, 1-8 (2017).
- [8] W. Park, E.Y. Choi, S.W. Kim, S.C. Jeon, Y.H. Cho, and J.M. Hur, "Electrolytic Reduction of a Simulated Oxide

- Spent Fuel and the Fates of Representative Elements in a  $\text{Li}_2\text{O}$ - $\text{LiCl}$  Molten Salt”, *J. Nucl. Mater.*, 477, 59-66 (2016).
- [9] I.S. Kim, S.C. Oh, H.S. Im, J.M. Hur, and H.S. Lee, “Distillation of  $\text{LiCl}$  From the  $\text{LiCl}$ - $\text{Li}_2\text{O}$  Molten Salt of the Electrolytic Reduction Process”, *J. Radioanal. Nucl. Chem.*, 295(2), 1413-1417 (2013).
- [10] E.Y. Choi, M.K. Jeon, and J.M. Hur, “Reoxidation of Uranium in Electrolytically Reduced Simulated Oxide Fuel During Residual Salt Distillation”, *J. Radioanal. Nucl. Chem.*, 314(1), 207-213 (2017).
- [11] M.K. Jeon, T.S. Yoo, E.Y. Choi, and J.M. Hur, “Quantitative Calculations on the Reoxidation Behavior of Oxide Reduction System for Pyroprocessing”, *J. Radioanal. Nucl. Chem.*, 313(1), 155-159 (2017).
- [12] E.Y. Choi, M.K. Jeon, S.W. Kim, and S. Paek, “Dilution of  $\text{Li}$ - $\text{Li}_2\text{O}$  in a Metallic Fuel Produced Through Oxide Reduction Using  $\text{ZrO}_2$ -assisted Rinsing in Molten  $\text{LiCl}$ ”, *J. Nucl. Mater.*, 533, 152107 (2020).
- [13] Y. Sakamura, M. Iizuma, S. Kitawaki, A. Nakayoshi, and H. Kofuji, “Formation and Reduction Behaviors of Zirconium Oxide Compounds in  $\text{LiCl}$ - $\text{Li}_2\text{O}$  Melt at 923 K”, *J. Nucl. Mater.*, 466, 269-279 (2015).
- [14] E.Y. Choi and D.H. Heo, “Reduction of Zirconium Oxide Compounds by Lithium Metal as a Reductant in Molten  $\text{LiCl}$  Salt”, *J. Nucl. Mater.*, 512, 193-198 (2018).
- [15] A. Roine, “Outokumpu HSC Chemistry® for Windows”, Version. 9.5.1, Metso Outotec Finland Oy, Locomonkatu 3, P.O. Box 306, FI-33101, Tampere, Finland (2018).